

Aza-Michael Reaction as a Route to Glycoconjugation of PETIM Dendrimers and Specificities of Bacterial Growth Inhibitions by Dendritic Glycoconjugates

Biswajit Sarkar,^a Avisek Mahapa,^{*,b,c} Kalyan Dey,^a Rakshit Manhas,^c Dipankar Chatterji,^{*,b}

Narayanaswamy Jayaraman^{*,a}

^a Department of Organic Chemistry, ^b Molecular Biophysics Unit, Indian Institute of Science, Bangalore 560 012, India, ^c Infectious Disease Department, CSIR-Indian Institute of Integrative Medicine, Jammu -180001, India.

Supporting Information

| S. No. | Content | Page |
|---------------|---|-------------|
| 1. | General information | S2 |
| 2. | Figure S1. ¹ H NMR spectrum of 2 | S4 |
| 3. | Figure S2. ¹³ C NMR spectrum of 2 | S4 |
| 4. | Figure S3. ESI-MS spectrum of 3 | S5 |
| 5. | Figure S4. ¹ H NMR spectrum of 3 | S5 |
| 6. | Figure S5. ¹³ C NMR spectrum of 3 | S6 |
| 7. | Figure S6. ¹ H NMR spectrum of 4 | S6 |
| 8. | Figure S7. ¹³ C NMR spectrum of 4 | S7 |
| 9. | Figure S8. MALDI-MS spectrum of 5 | S7 |
| 10. | Figure S9. ¹ H NMR spectrum of 5 | S8 |
| 11. | Figure S10. ¹³ C NMR spectrum of 5 | S8 |
| 12. | Figure S11. ¹ H NMR spectrum of 6 | S9 |
| 13. | Figure S12. ¹³ C NMR spectrum of 6 | S9 |
| 14. | Figure S13. ¹ H NMR spectrum of 7 | S10 |

| | | |
|----|---|-----|
| 15 | Figure S14. ^{13}C NMR spectrum of 7 | S10 |
| 16 | Figure S15. ^1H NMR spectrum of 8 | S11 |
| 17 | Figure S16. ^{13}C NMR spectrum of 8 | S11 |
| 18 | Figure S17. ^1H NMR spectrum of 9 | S12 |
| 19 | Figure S18. ^{13}C NMR spectrum of 9 | S12 |
| 20 | NMR characterization of amine-terminated PETIM dendrimers | S13 |
| 21 | Figures S19-S21. $-\ln[\text{Amine}]$ vs time plot for bis-amine glycoconjugation at varying temperature | S14 |
| 22 | Figures S22-S24. $-\ln[\text{Amine}]$ vs time plot for G1-amine glycoconjugation at varying temperature | S15 |

General information

Solvents were dried and distilled according to literature procedures. Chemicals were purchased from commercial sources and were used without further purifications. Silica gel (100-200 mesh) was used for column chromatography and TLC analysis was performed on commercial plates coated with silica gel 60 F254. Visualization of the spots on TLC plates was achieved by UV radiation or spraying 5 % sulphuric acid in ethanol.

Nuclear magnetic resonance spectra: ^1H and ^{13}C NMR spectra were recorded on Bruker 400 MHz NMR spectrometer and Jeol ECX500 NMR spectrometer. ^1H NMR spectra were referenced to CDCl_3 (7.26 ppm) or CD_3OD (3.31 ppm) whereas ^{13}C NMR spectra were referenced to CDCl_3 (77.0 ppm) or CD_3OD (49.0 ppm). Peak multiplicities are designated by the following abbreviations: s, singlet; br s, broad singlet; d, doublet; t, triplet; q, quartet; m, multiplet; dd, doublet of doublets; ddd, doublet of doublet of doublets. All the NMR spectra were recorded at 298 K. All the NMR data were analysed using Bruker TopSpin 3.6.2, Delta 5.3.1 and MestReNova as the data were collected from different NMR spectrometer and used according to the convenient.

Mass spectrometry: HRMS data were recorded on Bruker Daltonics MicroTOF-Q-II with electrospray ionization (ESI). MALDI-TOF/TOF mass spectrometry was performed with Bruker Daltonics UltrafleXtreme.

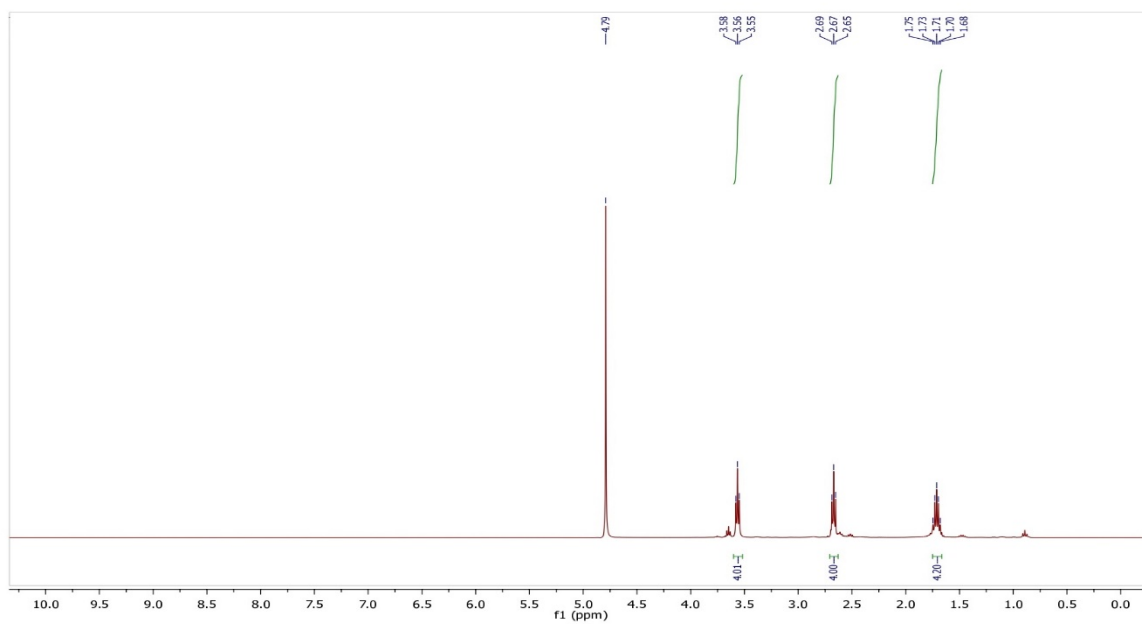


Figure S1. ¹H NMR spectrum of **2** (D₂O, 400 MHz).

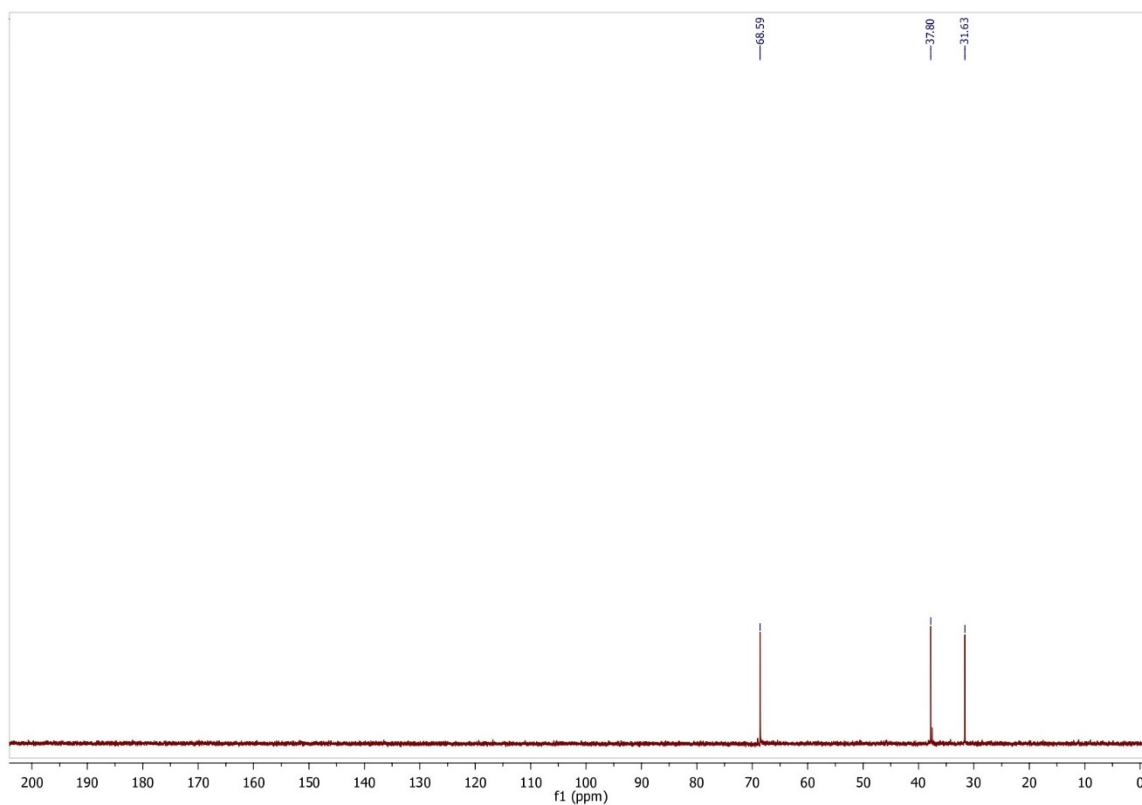


Figure S2. ¹³C NMR spectrum of **2** (D₂O, 100 MHz).

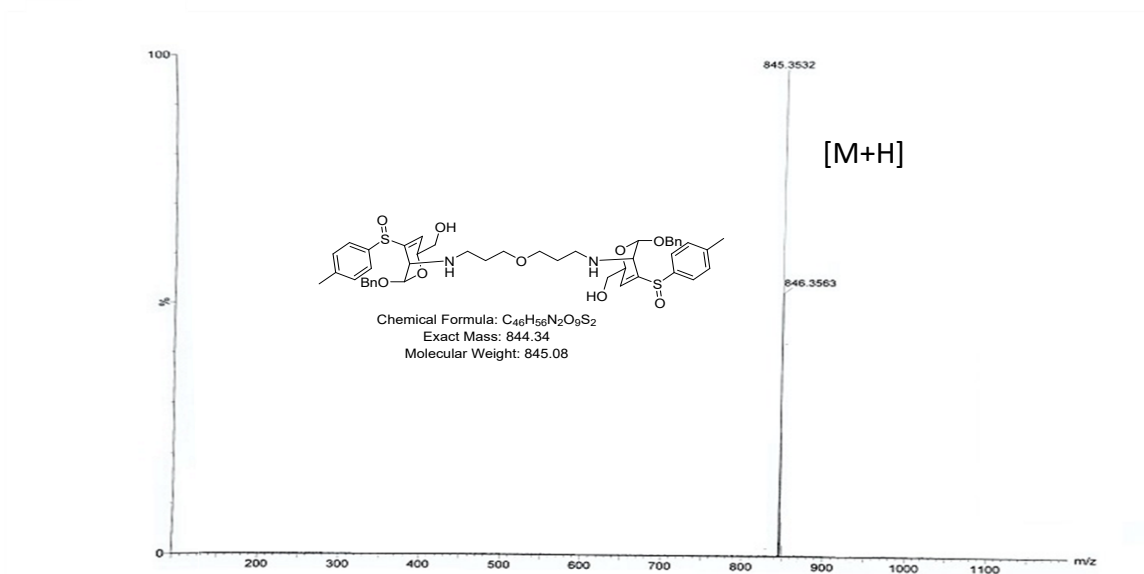


Figure S3. ESI-MS spectrum of **3**.

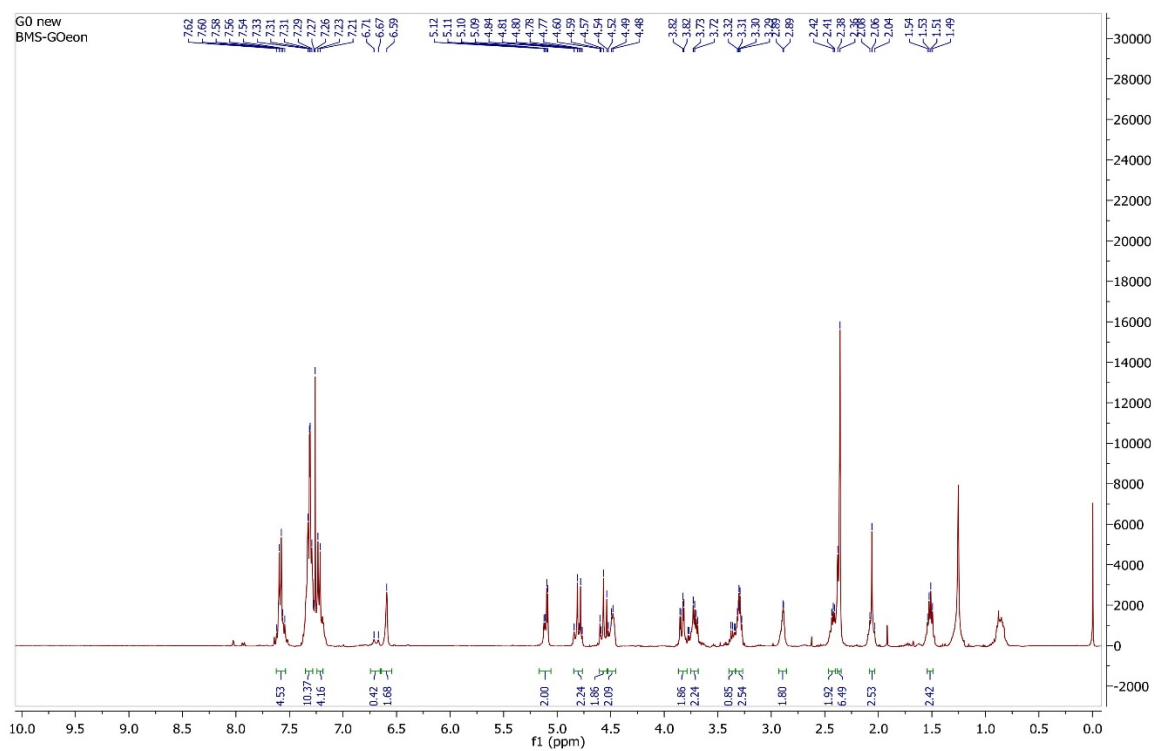


Figure S4. ¹H NMR spectrum of **3** (CDCl₃, 400 MHz).

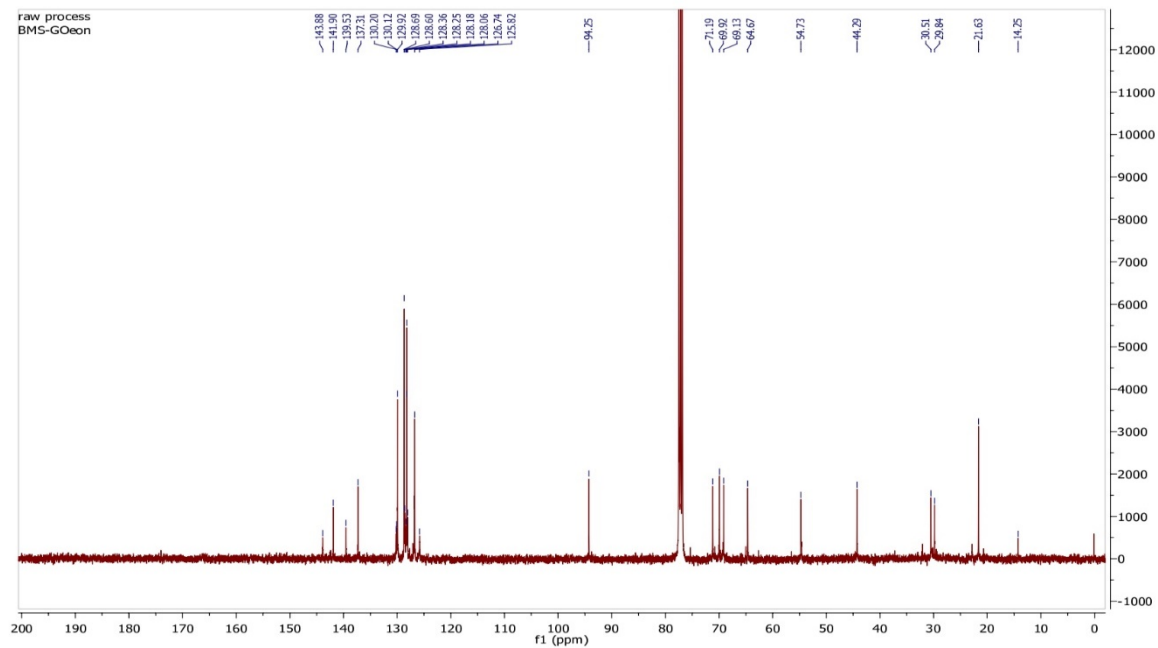


Figure S5. ^{13}C NMR spectrum of **3** (CDCl_3 , 100 MHz).

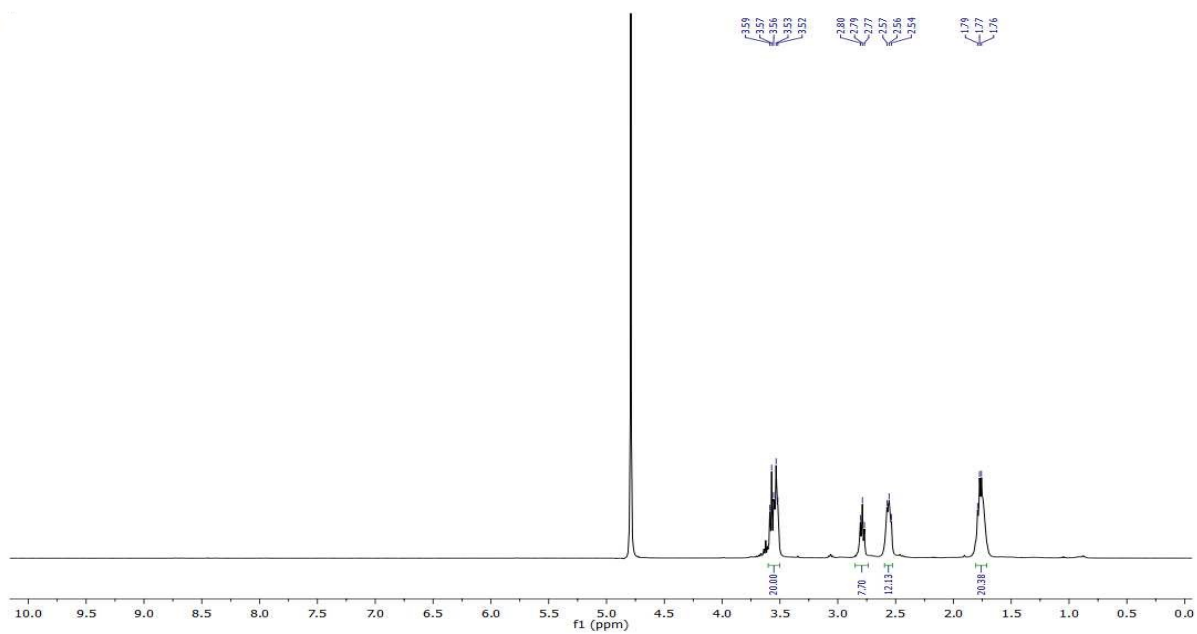


Figure S6. ^1H NMR spectrum of **4** (D_2O , 400 MHz).

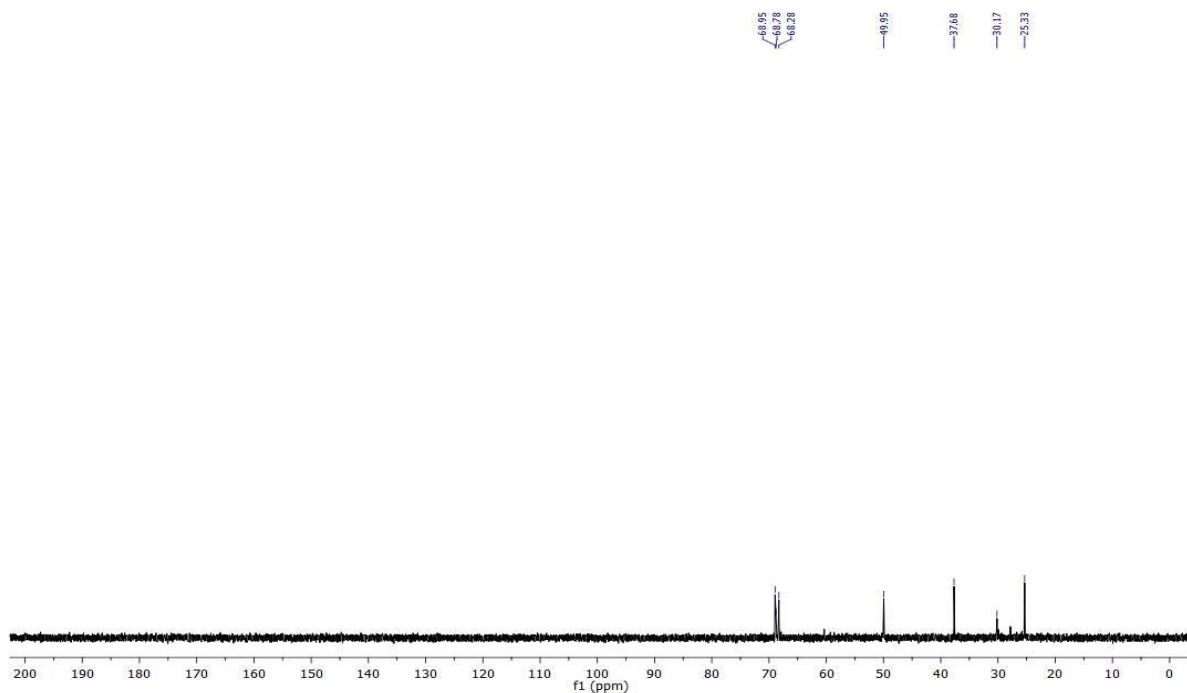


Figure S7. ^{13}C NMR spectrum of **4** (D_2O , 100 MHz).

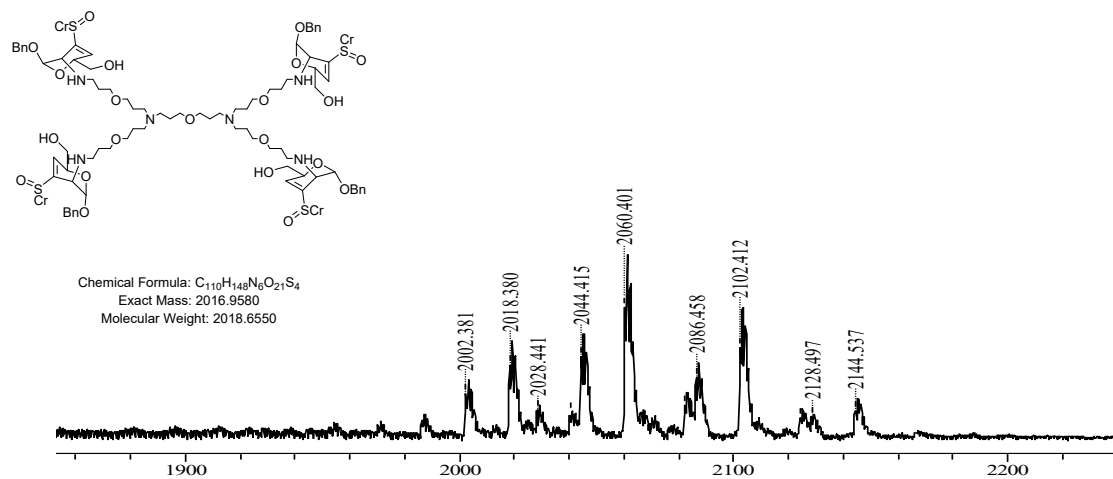


Figure S8. MALDI-MS spectrum of **5**.

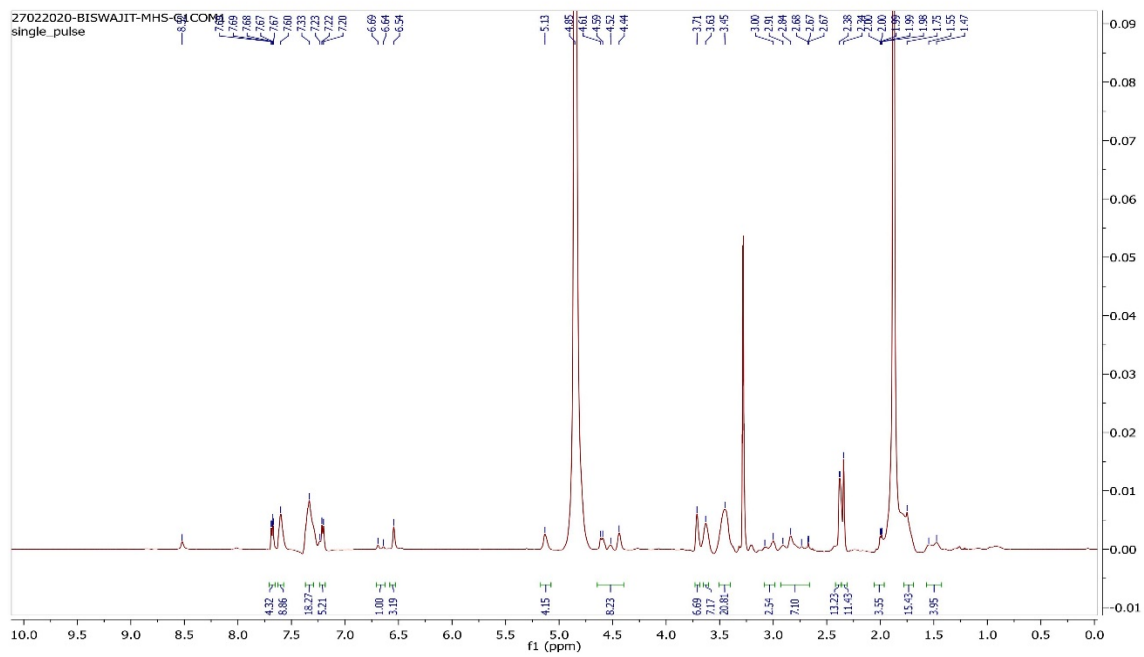


Figure S9. ^1H NMR spectrum of **5** (CD_3OD , 500 MHz).

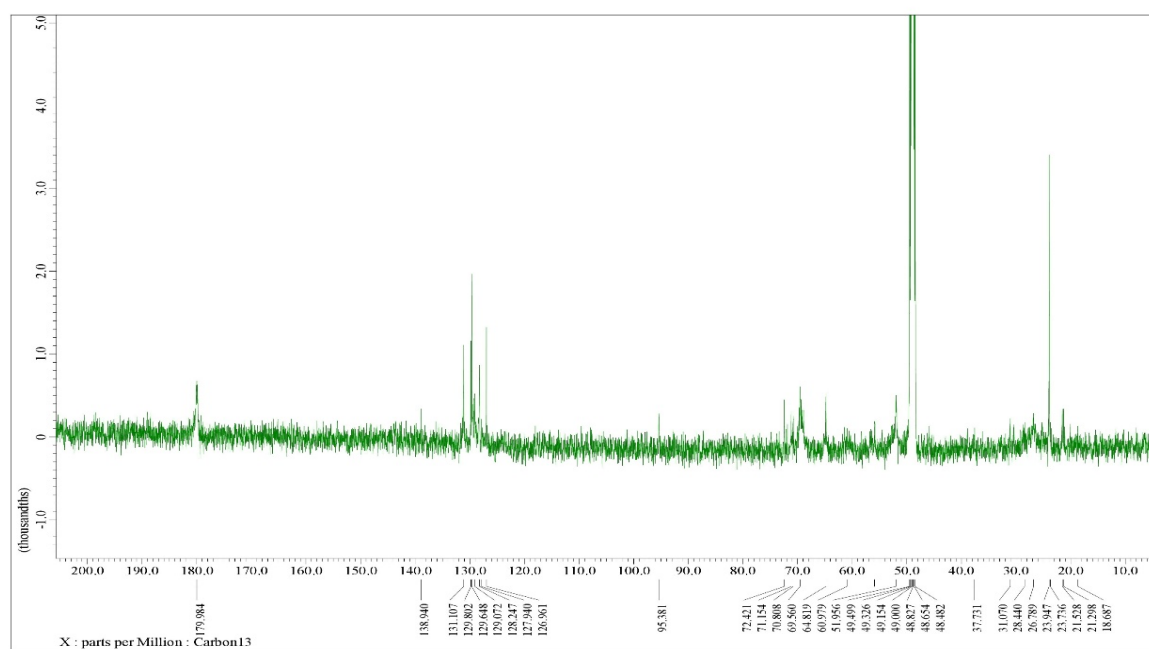


Figure S10. ^{13}C NMR spectrum of **5** (CD_3OD , 125 MHz).

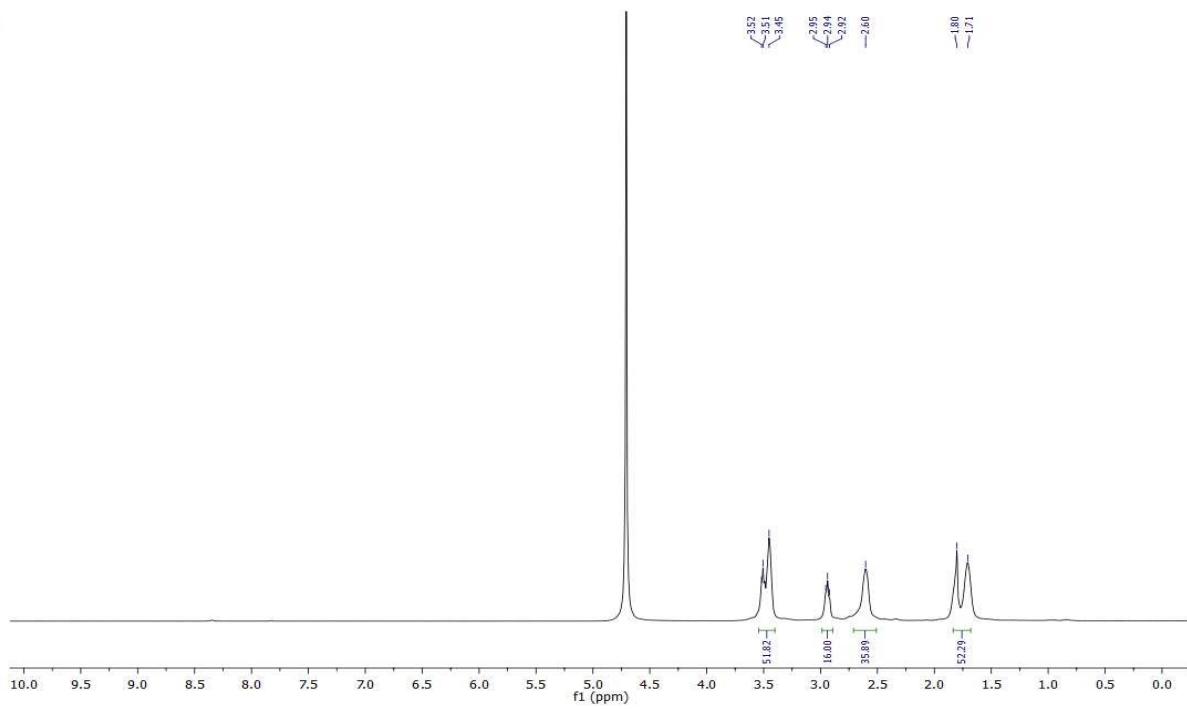


Figure S11. ¹H NMR spectrum of **6** (D₂O, 400 MHz).

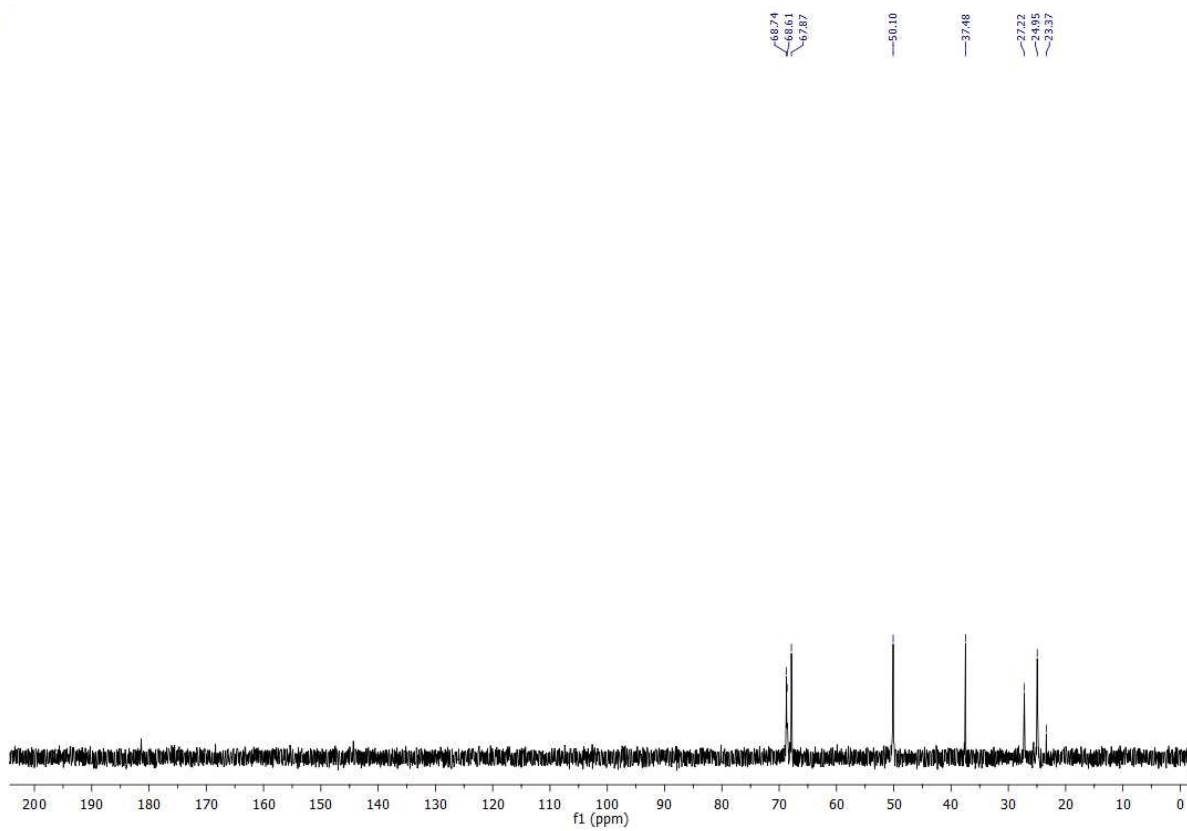


Figure S12. ¹³C NMR spectrum of **6** (D₂O, 100 MHz).

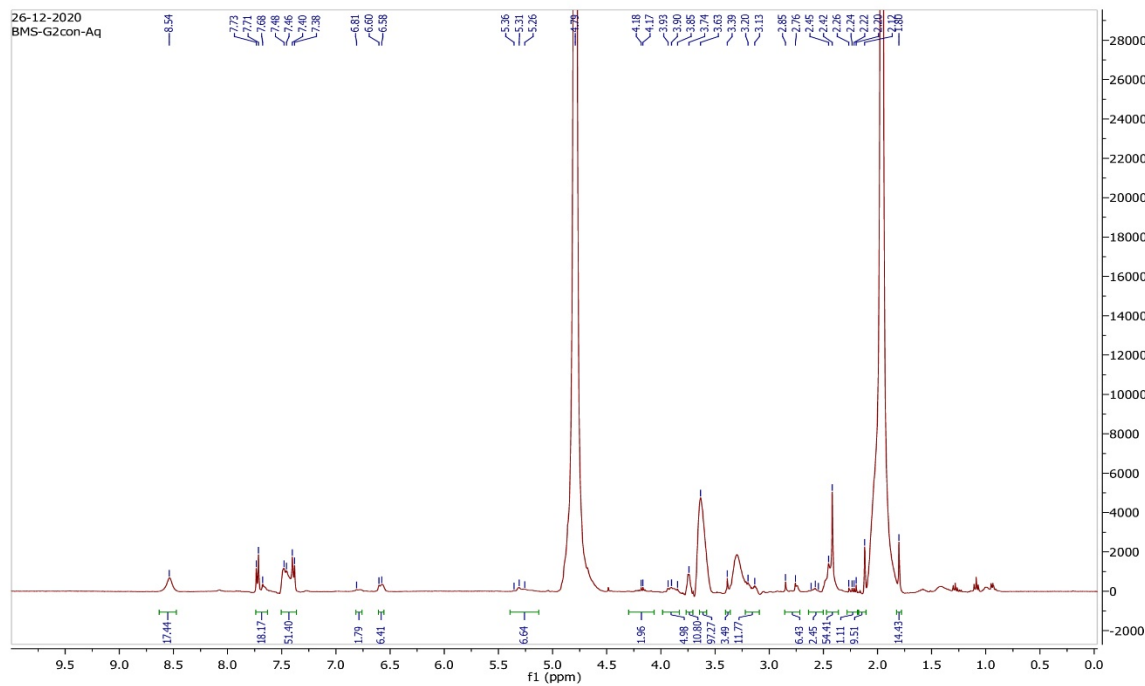


Figure S13. ^1H NMR spectrum of **7** (CD_3OD , 500 MHz).

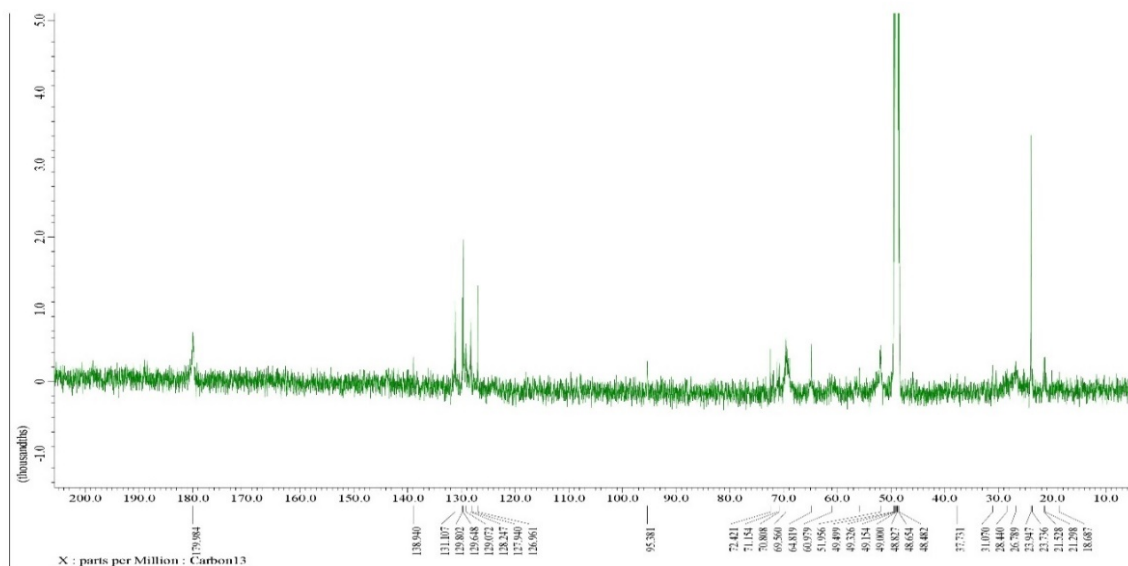


Figure S14. ^{13}C NMR spectrum of **7** (CD_3OD , 125 MHz).

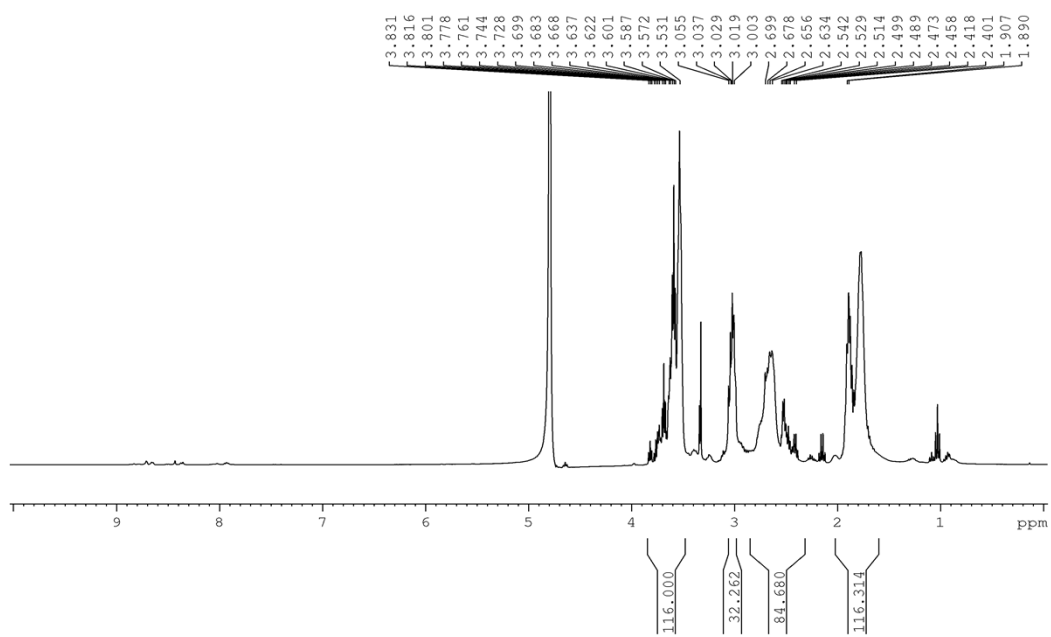


Figure S15. ^1H NMR spectrum of **8** (D_2O , 400 MHz).

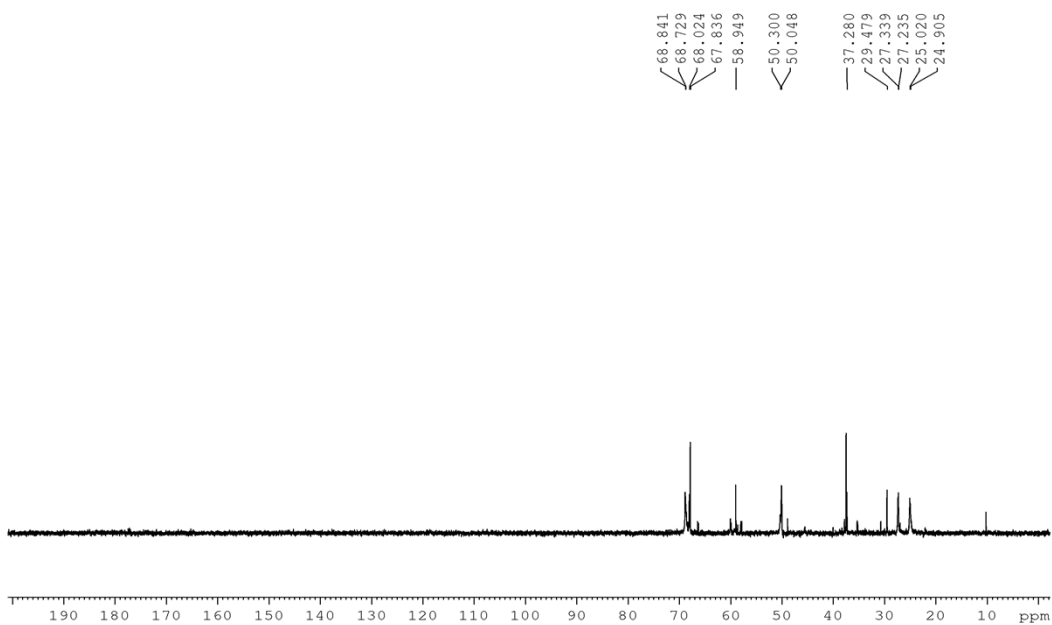


Figure S16. ^{13}C NMR spectrum of **8** (D_2O , 100 MHz).

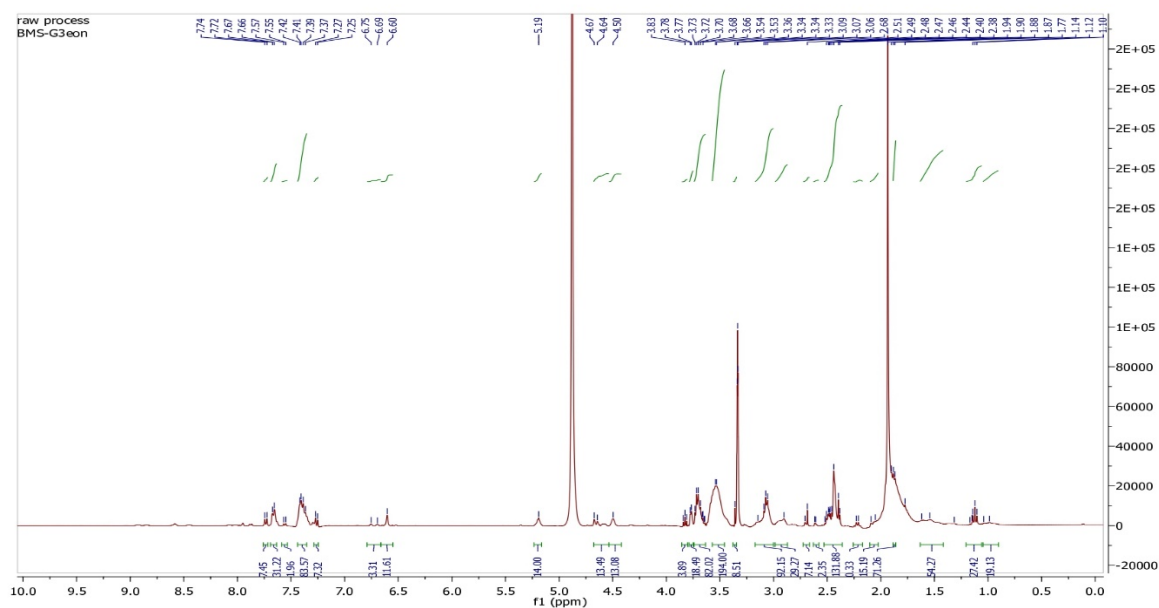


Figure S17. ^1H NMR spectrum of **9** (CD_3OD , 400 MHz).

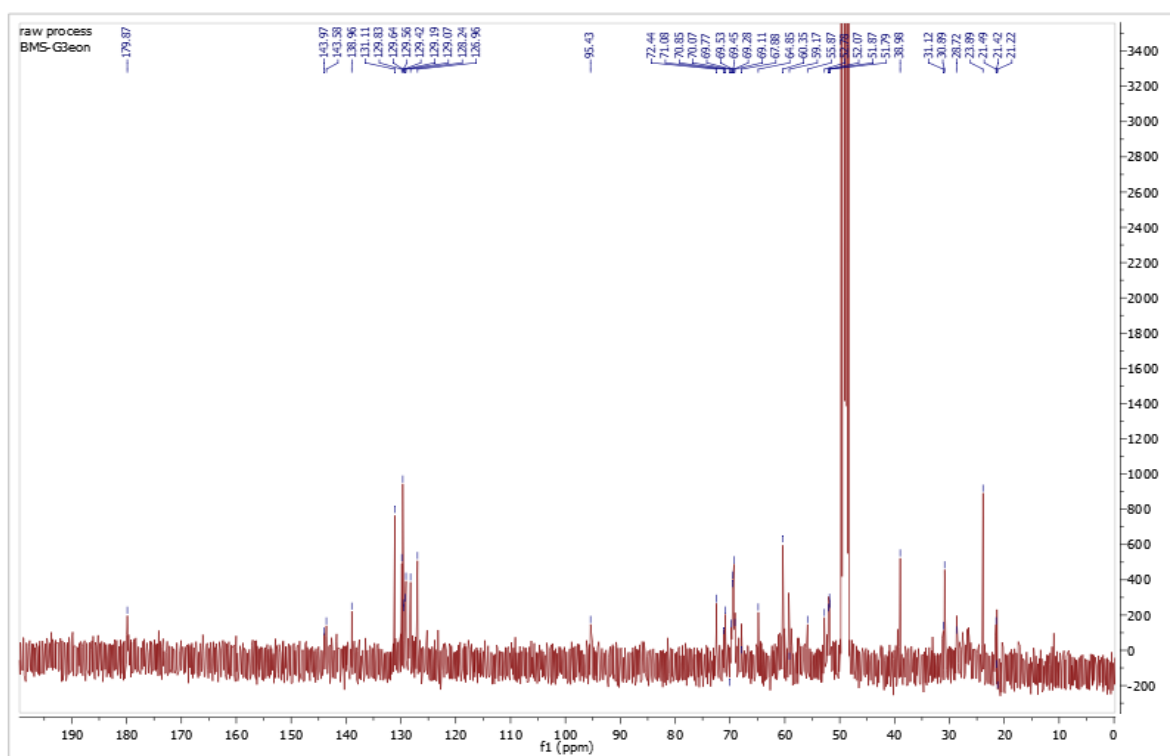


Figure S18. ^{13}C NMR spectrum of **9** (CD_3OD , 100 MHz).

20. ^1H and ^{13}C NMR spectral characterization of amine terminated PETIM dendrimer

G0-(NH₂)₂: ^1H NMR (400 MHz, D₂O): δ 3.56 (t, J = 4 Hz, 4 H, -OCH₂), 2.67 (t, J = 8 Hz, 4 H, -NCH₂-), 1.75-1.68 (app. m, 4 H, -CH₂-); ^{13}C NMR (100 MHz, D₂O): δ 68.6 (-OCH₂-), 37.8 (-NCH₂-), 31.6 (-CH₂-).

G1-(NH₂)₄ (4): ^1H NMR (400 MHz, D₂O): δ 3.59-3.52 (m, 20 H, -OCH₂), 2.79 (t, J = 8 Hz, 8 H, CH₂-NH₂), 2.56 (t, J = 8 Hz, 12 H, -NCH₂-), 1.77 (t, J = 8 Hz, 20 H, -CH₂-); ^{13}C NMR (100 MHz, D₂O): δ 68.9, 68.8, 68.3 (-OCH₂-), 49.9 (-NCH₂-), 37.7 (CH₂-NH₂), 30.2, 25.3 (-CH₂-).

G2-(NH₂)₈ (6): ^1H NMR (400 MHz, D₂O): δ 3.52-3.45 (m, 52 H, -OCH₂), 2.94 (t, J = 8 Hz, 16 H, CH₂-NH₂), 2.60 (br. s, 36 H, -NCH₂-), 1.80-1.71 (br. m, 52 H, -CH₂-); ^{13}C NMR (100 MHz, D₂O): δ 68.7, 68.6, 67.8 (-OCH₂-), 50.1 (-NCH₂-), 37.5 (CH₂-NH₂), 27.2, 24.9, 23.4 (-CH₂-).

G3-(NH₂)₁₆ (8): ^1H NMR (400 MHz, D₂O): δ 3.83-3.53 (m, 116 H, -OCH₂), 3.05-3.00 (m, 32 H, CH₂-NH₂), 2.69-2.40 (br. m, 84 H, -NCH₂-), 1.90-1.89 (br. m, 116 H, -CH₂-); ^{13}C NMR (100 MHz, D₂O): δ 68.8, 68.7, 68.0, 67.8 (-OCH₂-), 58.9, 50.3, 50.0 (-NCH₂-), 37.3 (CH₂-NH₂), 29.5, 27.3, 27.2, 25.0, 24.9 (-CH₂-).

21. $-\ln[\text{Amine}]$ vs time plot for kinetics experiment

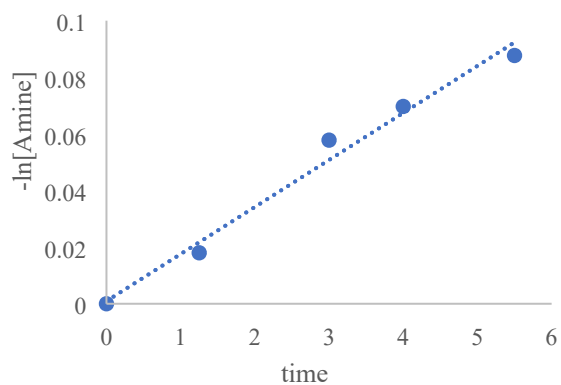


Figure S19. $-\ln[\text{Amine}]$ vs time plot for bis-amine glycoconjugation at 25 °C.

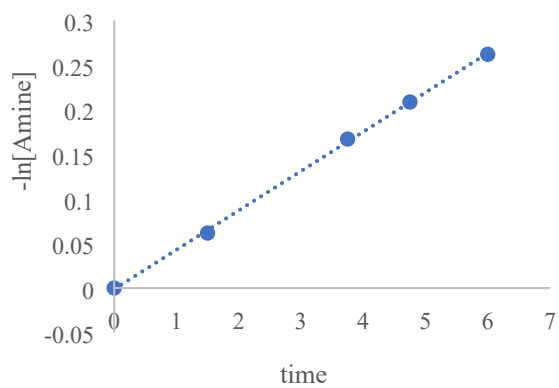


Figure S20. $-\ln[\text{Amine}]$ vs time plot for bis-amine glycoconjugation at 35 °C.

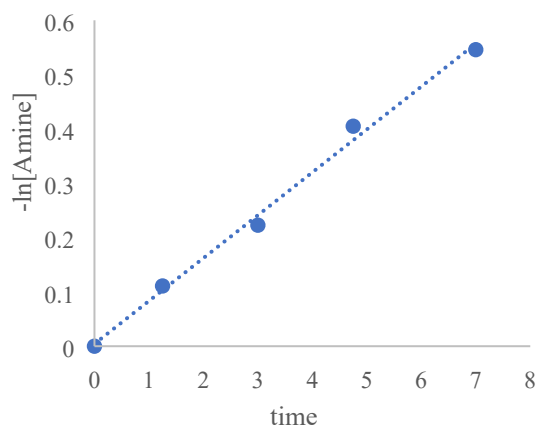


Figure S21. $-\ln[\text{Amine}]$ vs time plot for bis-amine glycoconjugation at 45 °C.

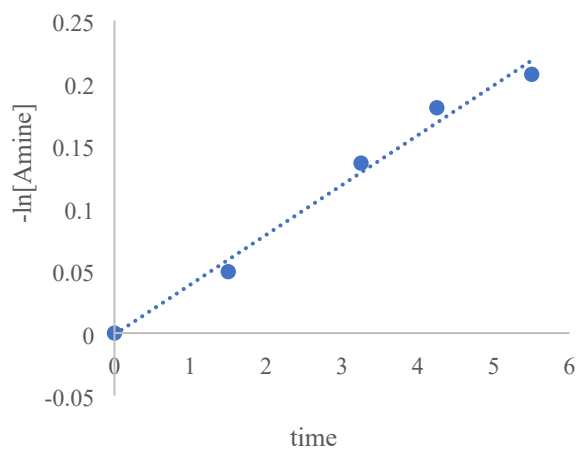


Figure S22. $-\ln[\text{Amine}]$ vs time plot for G1-amine glycoconjugation at 25 °C.

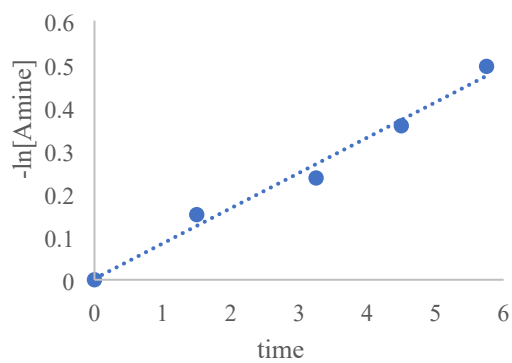


Figure S23. $-\ln[\text{Amine}]$ vs time plot for G1-amine glycoconjugation at 35 °C.

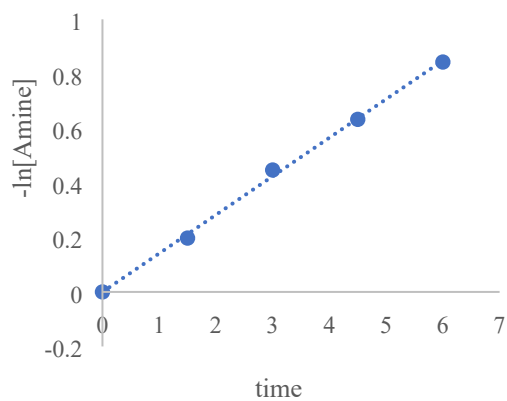


Figure S24. $-\ln[\text{Amine}]$ vs time plot for G1-amine glycoconjugation at 45 °C.